Loss of Stability in a Small-Caliber Vascular Graft

©

K.U. Klyshnikov, Researcher, Laboratory of New Biomaterials, Experimental
and Clinical Cardiology Department;
E.A. Ovcharenko, PhD, Head of the Laboratory of New Biomaterials, Experimental
and Clinical Cardiology Department;
M.A. Rezvova, Junior Researcher, Laboratory of New Biomaterials, Experimental
and Clinical Cardiology Department;
T.V. Glushkova, PhD, Researcher, Laboratory of New Biomaterials, Experimental
and Clinical Cardiology Department;
V.V. Sevostyanova, PhD, Researcher, Laboratory of Cell Technologies, Experimental
and Clinical Cardiology Department;
L.V. Antonova, PhD, Head of the Laboratory of Cell Technologies, Experimental
and Clinical Cardiology Department;
Yu.A. Kudryavtseva, DSc, Head of Experimental and Clinical Cardiology Department;
L.S. Barbarash, MD, DSc, Professor, Academician of the Russian Academy of Sciences, Chief Researcher

Research Institute for Complex Issues of Cardiovascular Diseases, 6 Sosnovy Blvd, Kemerovo,
650002, Russia

The aim of the study is to develop and test a numerical method for assessing a loss of stability in a polymer vascular graft in response to a longitudinal dynamic high-speed load.

Materials and Methods. A small-caliber vascular graft made by electrospinning from the composite mixture of polyhydroxybutyrate/valerate and polycaprolactone polymers was studied. Numerical methods (finite element method) and prototype test (uniaxial tension) were used to assess the loading speeds and the resulting loss of stability, which are critical for small-caliber vascular grafts.

Results. The mechanical testing of a vascular graft prototype allowed us to determine its response to quasi-static load. We also showed that the high-speed longitudinal dynamic loads significantly reduced the load-carrying capacity of the structure. This and related effects are suggested to be potential causes of the vessel lumen collapse resulted from irreversible loss of stability.

Conclusion. The impact of a dynamic load significantly weakens the vascular graft and affects its elastic and deformation characteristics, leading to the premature critical deformation and eventual occlusion. Therefore, the quality of such products can be improved by a preliminary prognostic work and reinforcement of their construction.

Key words: computer simulation; vascular graft; loss of stability in vascular graft; frequency analysis.

Introduction

From the engineering point of view, a significant number of medical devices used in cardiovascular surgery are thin-walled cylinders resembling the "tubular" structure of blood vessels [1]. Vascular prostheses, coronary and peripheral stents, transcatheter heart valve prostheses, and other minimally invasive devices can be included in this group [2, 3]. As far as the design is concerned, the description of these objects as hollow cylinders greatly simplifies the modeling and calculating processes [4]. However, a number of factors such as the complicated geometry of medical devices, their complex macro- and microstructure, and the non-linear quality of their materials do not allow for an analytical solution to the problems of strength, fatigue and, therefore, reliability of these products. To tackle these problems, numerical analysis of medical objects — prosthetic

---

Corresponding author: Kirill U. Klyshnikov, e-mail: Klyshnikovk@gmail.com

heart valves, stents, vessels — has been developed; this approach is based on the finite element method that takes into account the nonlinear characteristics (geometrical, mechanical, structural), varying loads and the multi-component structure of medical devices [5, 6].

Among the family of thin-walled cylindrical shells, there are prostheses for peripheral and central sections of the vascular bed, i.e. polymeric or biological (allo- or xenoimplants) tubular medical devices implanted into blood vessels for a long time. During their life-time these implants are acted upon by multidirectional loads — radial (torsion) and longitudinal (extension/compression), including dynamic loads [7–9]. In the studies world-wide, the high-speed loads on the grafts are rarely taken into account, although such phenomena may occur during surgery and have consequences different from those under quasi-static loads [10, 11].

In this study, we aimed to evaluate the response (i.e. a loss of stability) of a small-caliber vascular prosthesis to a high-speed axial dynamic load.

Materials and Methods

We developed and tested a numerical method for assessing the response of a vascular graft to the dynamic high-speed load.

Object of study. We used a vascular biodegradable graft with a diameter of 4 mm and a wall thickness of 0.35 mm made by electrospinning from a mixture of polyhydroxybutyrate/valerate copolymer with a valerate content of at least 8% (PHBV; Sigma-Aldrich, USA) and polycaprolactone with a molecular mass of 80 kDa (PCL; Sigma-Aldrich, USA) in chloroform (Vekton, Russia) [12]. The average fiber diameter was 0.240 µm, the pore area

was 1.419 µm^2, and the porosity of the material was 49.75%. The outer surface of the graft was covered with a spiral reinforcing thread with a diameter of 0.3 mm, made of the same 80 kDa polycaprolactone using the method of extrusion.

Three-dimensional model of the graft. The 3D model of the small-caliber vascular graft consists of a hollow cylinder of a constant cross-section area; the structure is equipped with a reinforcing coil. The model was created in the NX design environment (Germany), using the tools of 2D and 3D object construction. The wall thickness of the cylindrical part was 0.3 mm, the thickness of the reinforcing coil was 0.3 mm, the soldering depth was 50%, and the length of the graft was 60 mm.

By exporting the above characteristics to the *.step format, a transfer of the graft geometry to the Abaqus/CAE 6.14 (USA) software had been accomplished; there, the study on the loss of stability continued. The imported model became the basis for creating a tetrahedral grid based on four-node elements of the first order interpolation — tetrahedral, C3D4 (n=181,195 elements) [13]. The resulting finite element mesh (Figure 1 (a)) was used without changes at all stages: the natural frequency analysis and the loss of stability modeling.

Analysis of natural frequencies. To select the critical values of loading speeds for the subsequent modeling and mechanical testing, we conducted a search for natural frequencies underlying the resonance phenomena, which may lead to a loss of stability. The problem was approached by running the frequency analysis in the Abaqus/CAE 6.14 (USA) environment based on the Lanczos solver with a limit for the maximum frequency at 1000 Hz. The degrees of freedom of the end nodes of the graft were connected with control points (CP) — CP1 and CP2. These limiting conditions and loads were applied to the given reference points followed by their transfer through the created kinematic constraint onto the nodes of the associated end sections. The limiting conditions were defined as follows: complete restriction for all degrees of freedom for the proximal CP1 (0; 0; 0), and, therefore, for all nodes connected with it. For the distal CP2 (0; 0; 60), similar restrictions were chosen, except for the free longitudinal movement:

$$U(CP1)_i=0, \; i=1, ..., 6;$$
$$U(CP2)_i=0, \; i=1, 2, 4, 5, 6.$$

The experimental design with the imposed limiting conditions is shown in Figure 1.

In the literature [14], it has been shown that the linearized approach to the loss of stability model significantly underestimates the forces causing this phenomenon, despite the qualitative similarity between the deformation results. Therefore, we studied a nonlinear response by the elastoplastic material model and the respective geometric nonlinearity. The behavior
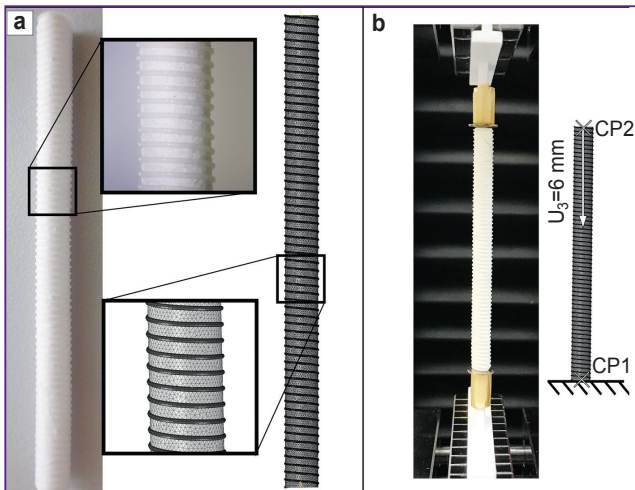

Figure 1. Materials used:
(a) study object, a small-caliber vascular graft (*left*) and a 3D finite element model for subsequent computations (*right*); (b) experiment on the of loss of stability: prototype (*left*) and numerical (*right*); CP — control point, U$_3$ — longitudinal movement

K.U. Klyshnikov, E.A. Ovcharenko, M.A. Rezvova, T.V. Glushkova, V.V. Sevostyanova, …, L.S. Barbarash

of the material was described by an elastoplastic model with isotropic hardening, with the von Mises yield factor, and with parameters obtained in our earlier studies [15] (see the Table).

The values of natural frequencies obtained in this analysis (the first three forms) were used to calculate the loading speed in our prototype experiment and in the loss of stability modeling. To this end, the resulting natural oscillation frequency was recalculated into the time units (s) and, by setting the traverse movement of the universal testing machine to 6 mm (10% of the graft length), the movement speed (mm/s) leading to a loss of stability was calculated. In total, three natural oscillation frequencies were obtained; those referred to three speeds of axial loading on the grafts, which caused a loss of stability in three different forms.

Mechanical tests. The accuracy of numerical experiments largely depends on the qualitative characteristics of the material and their interpretation in the model. The solutions were sought by applying a uniaxial compression using a universal Z-series testing machine (Zwick Roell, Germany) in accordance with ISO 7198–2013. We used a sensor with a nominal value of 50 N and with a measurement error of 1%. The traverse speed was 10 mm/min, and the path length was 6 mm, which was 10% of the entire graft length. Using this test, we evaluated the qualitative and quantitative characteristics of the response in terms of strain–deformation and force–displacement curves. Thus, the quasi-static (slow) reaction of the graft was investigated.

Numerical simulation. The loss of stability was evaluated in a prototype and numerical experiments under the respective limiting conditions (see Figure 1). For the numerical simulation, we chose the dynamics method based on the Abaqus/Explicit solver algorithm [16, 17]. The algorithm includes an explicit scheme of integrating equations that describe the time-dependent motion. Technically, the algorithm provides for solving the below equation with a diagonal mass matrix of each element:

$$a = M^{-1}(P - I),$$

where a is the acceleration of the model nodes; M is the diagonal mass matrix of each element; P — the external forces; I — the internal forces.

Specifics of numerical solutions by the finite element method of dynamic problems associated with a small time increment for each step, especially for high-precision grids, led us to use an artificial mass scaling. The value of the scaling parameter was selected considering the need to comply with the requirement of not exceeding the 5% contribution of kinetic energy to the potential energy of the system. Such an approach allows for controlling the contribution of the inertial component [18, 19].

Characteristics of materials used in the numerical calculation

Material	E (MPa)	ν (m/m)	Plastic deformation							
			σ_1	ε_1	σ_2	ε_2	σ_3	ε_3	σ_4	ε_4
Base	1.7	0.3	1.0	0.0	1.5	0.2	3.0	0.9	6.0	1.5
Coil	350.0	0.3	—	—	—	—	—	—	—	—

N o t e: E — the modulus of elasticity; ν — the Poisson' ratio; σ — the point determining the strain in the plastic response zone; ε — the point determining the deformation of the plastic response zone.

Results

Mechanical tests. The prototype experiment on quasi-static compression of the graft resulted in a zonal response to the applied load (Figure 2). The zone of elastic reversible deformation *1* is characterized by a sharp increase in the force with a small increase in the deformation. The subsequent transition *2* represents the beginning of irreversible structural changes, i.e. the plastic deformation. A sharp increase *3* in deformations with a small increase in force represents the plastic response zone. The obtained force–deformation and strain–deformation curves were used to determine the constants of the material through the numerical simulation.

Numerical simulation

Analysis of natural frequencies. The values of natural frequencies obtained at the first stage were: 32.9, 43.0, and 83.4 Hz for the first three forms of the loss of stability (Figure 3). Based on these data, the threshold values of the loading speed were calculated for the subsequent numerical experiment considering the displacement of 10% (6 mm). In order to simulate the loss of stability for each of the forms, the following speed values were obtained: 198.0, 258.6, and 500.8 mm/s.

Modeling the loss of stability. The numerical analysis of the stability loss resulted in the force–deformation curves that were zonal in nature. Thus, with
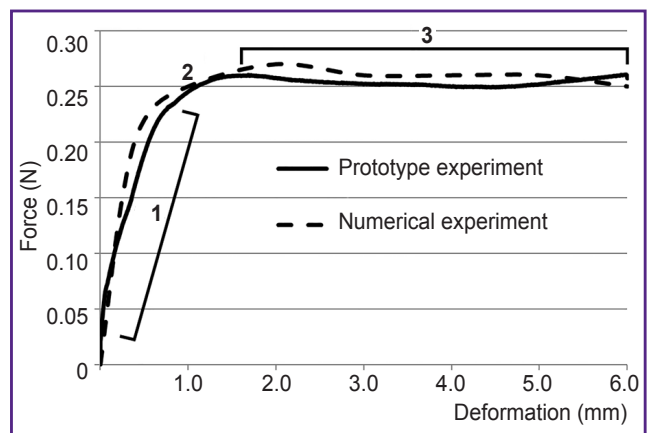
Figure 2. Mechanical properties of the studied graft, as resulted from the prototype experiment and the numerical simulation
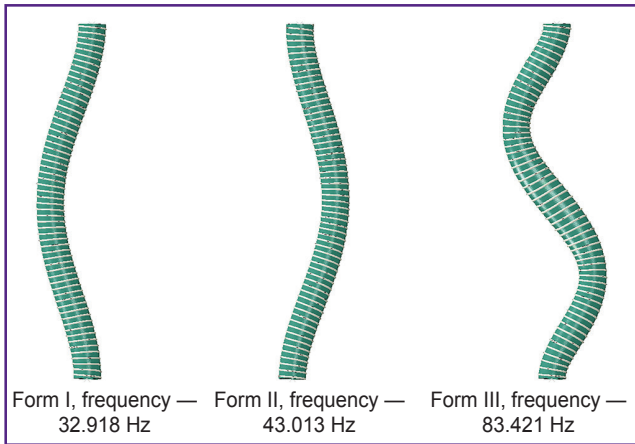See explanations in the text

Figure 3. Forms of the stability loss (I, II, and III) in a reinforced vascular graft resulted from the natural frequencies analysis
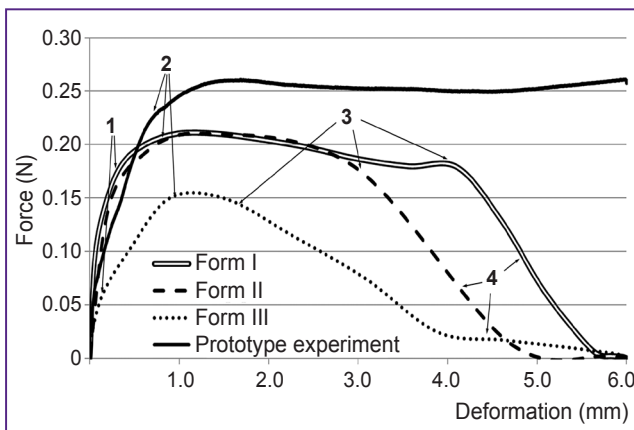

Figure 4. Results of numerical modeling of the dynamic and quasi-static loads in the prototype experiment:
1 — zone of elastic reversible deformation; *2* — transition to the zone of plastic irreversible deformation; *3* — loss of structural stability; *4* — zone of decreasing bearing capacity of the graft

an increasing displacement under fast loading, the force distribution could be classified into: elastic deformation zone *1*, irreversible plastic deformation zone *2*, loss of stability *3*, and a subsequent sharp decrease in the bearing capacity *4* (Figure 4). In modeling the loss of stability of forms I, II, and III, we determined force peaks (i.e. the limit values of bearing capacity) at 0.225, 0.211, and 0.152 N, respectively. Notably, the prototype experiment on quasi-static loading produced a more stable response, where the maximal generated force varied from 0.2511 to 0.2601 N throughout the entire zone of irreversible deformations.

This series of numerical experiments demonstrated noticeable differences (qualitative and quantitative) in the mechanical response of the vascular graft to the quasi-static vs dynamic loads. Two characteristic features of the graft reaction under fast loading can be underscored:

1) a zonal character of the force–deformation curves, and 2) a decrease in the maximum force (the bearing capacity limit) toward values below the "slow" load levels. Such a behavior is due to the slow reaction of the graft material under high compression speeds, which is clearly demonstrated with the form III natural frequency, where the speed reaches extreme values of 500.8 mm/s. The drop in the maximum force, noted in all three cases of dynamic loading, and especially pronounced in the form III model, reaches 60.5% of the initial value.

Discussion

It is noteworthy that the response curve in subcritical regions *1* and *2* (see Figure 4) qualitatively resembles that of quasi-static loading, i.e. the elastic component approximating the plateau of irreversible deformation. It is important that the slope (actually the modulus of elasticity) in zone *1* is similar to that in the prototype experiment, i.e. the elastic component of the response does not undergo significant changes. The ranges *3* and *4* (which extend over the critical values) are qualitatively different and unique for this type of analysis as they demonstrate a change in the structure — significant weakening under the dynamic load. Considering the long-term functioning of a vascular graft in the patient's body (5–10 years), the probability of such dynamic loads may become relatively high [20].

Conclusion

A dynamic load on the small-caliber vascular graft significantly weakens its structure and also affects its mechanical characteristics, causing a premature critical deformation, which can result in a collapse of the lumen (occlusion) or irreversible deformation of the graft, reducing its cycle resistance. We suggest to improve the quality of such products by a preliminary prognostic work and reinforcement of their construction.

Conflict of interest. There is no conflict of interest.

References

1. Chen H., Kassab G.S. Microstructure-based constitutive model of coronary artery with active smooth muscle contraction. *Sci Rep* 2017; 7(1): 9339, https://doi.org/10.1038/s41598-017-08748-7.

2. Stankiewicz J.M., Robertson S.W., Ritchie R.O. Fatigue-crack growth properties of thin-walled superelastic

K.U. Klyshnikov, E.A. Ovcharenko, M.A. Rezvova, T.V. Glushkova, V.V. Sevostyanova, ..., L.S. Barbarash

austenitic Nitinol tube for endovascular stents. *J Biomed Mater Res A* 2007; 81(3): 685–691, https://doi.org/10.1002/jbm.a.31100.

3. Bernardini A., Larrabide I., Morales H.G., Pennati G., Petrini L., Cito S., Frangi A.F. Influence of different computational approaches for stent deployment on cerebral aneurysm haemodynamics. *Interface Focus* 2011; 1(3): 338–348, https://doi.org/10.1098/rsfs.2011.0004.

4. Lee A.Y., Han H.-C. A nonlinear thin-wall model for vein buckling. *Cardiovasc Eng* 2010; 1(4): 282–289, https://doi.org/10.1007/s13239-010-0024-4.

5. Suzuki T., Takao H., Fujimura S., Dahmani C., Ishibashi T., Mamori H., Fukushima N., Yamamoto M., Murayama Y. Selection of helical braided flow diverter stents based on hemodynamic performance and mechanical properties. *J Neurointerv Surg* 2017; 9(10): 999–1005, https://doi.org/10.1136/neurintsurg-2016-012561.

6. Li H., Gu J., Wang M., Zhao D., Li Z., Qiao A., Zhu B. Multi-objective optimization of coronary stent using Kriging surrogate model. *Biomed Eng Online* 2016; 15(Suppl 2): 148, https://doi.org/10.1186/s12938-016-0268-9.

7. Smouse H.B., Nikanorov A., LaFlash D. Biomechanical forces in the femoropopliteal arterial segment. What happens during extremity movement and what is the effect on stenting? *Endovasc Today* 2005; 4: 60–66.

8. Li H., Leow W.K., Chiu I.S. Modeling torsion of blood vessels in surgical simulation and planning. *Stud Health Technol Inform* 2009; 142: 153–158.

9. Selvaggi G., Anicic S., Formaggia L. Mathematical explanation of the buckling of the vessels after twisting of the microanastomosis. *Microsurgery* 2006; 26(7): 524–528, https://doi.org/10.1002/micr.20281.

10. Garcia J.R., Lamm S.D., Han H.-C. Twist buckling behavior of arteries. *Biomech Model Mechanobiol* 2013; 12(5): 915–927, https://doi.org/10.1007/s10237-012-0453-0.

11. Ding Z., Friedman M.H. Dynamics of human coronary arterial motion and its potential role in coronary atherogenesis. *J Biomech Eng* 2000; 122(5): 488–492, https://doi.org/10.1115/1.1289989.

12. Antonova L.V., Sevostyanova V.V., Velikanova E.A., Matveeva V.G., Glushkova T.V., Mironov A.V., Krivkina E.O., Barbarash L.S. Biofunctionalization of biodegradable small-diameter vascular grafts VEGF, BFGF, and SDF-1A: experimental results. *Vestnik transplantologii i iskusstvennykh organov* 2017; 19(5): 197.

13. Belytschko T., Bindeman L.P. Assumed strain stabilization of the eight node hexahedral element. *Comput Methods Appl Mech Eng* 1993; 105: 225–260, https://doi.org/10.1016/0045-7825(93)90124-g.

14. Nushtaev D.V., Zhavoronok S.I., Klyshnikov K.Y., Ovcharenko E.A. Combined numerical and experimental investigation of the deformed state and buckling of the meshed cylindrical shell subjected to the axial compression. *Trudy MAI* 2015; 82: 9.

15. Glushkova T.V., Sevostyanova V.V., Antonova L.V., Klyshnikov K.Yu., Ovcharenko E.A., Sergeeva E.A., Vasyukov G.Yu., Seifalian A.M., Barbarash L.S. Biomechanical remodeling of biodegradable small-diameter vascular grafts in situ. *Vestnik transplantologii i iskusstvennykh organov* 2016; 18(2): 99–109.

16. Belytschko T., Lin J.I., Tsay C.S. Explicit algorithms for the nonlinear dynamics of shells. *Comput Methods Appl Mech Eng* 1984; 42(2): 251–276, https://doi.org/10.1016/0045-7825(84)90026-4.

17. Xu J., Yang J., Huang N., Uhl C., Zhou Y., Liu Y. Mechanical response of cardiovascular stents under vascular dynamic bending. *Biomed Eng Online* 2016; 15(1): 21, https://doi.org/10.1186/s12938-016-0135-8.

18. Spranger K., Capelli C., Bosi G.M., Schievano S., Ventikos Y. Comparison and calibration of a real-time virtual stenting algorithm using finite element analysis and genetic algorithms. *Comput Methods Appl Mech Eng* 2015; 293: 462–480, https://doi.org/10.1016/j.cma.2015.03.022.

19. Fu W., Xia Q. Interaction between flow diverter and parent artery of intracranial aneurysm: a computational study. *Appl Bionics Biomech* 2017; 2017: 3751202, https://doi.org/10.1155/2017/3751202.

20. Antonova L.V., Krivkina E.O., Sergeeva E.A., Sevostyanova V.V., Burago A.Yu., Burkov N.N., Sharifulin R.F., Velikanova E.A., Kudryavtseva Yu.A., Barbarash O.L., Barbarash L.S. Tissue engineered scaffold modified by bioactive molecules for directed tissue regeneration. *Complex Issues of Cardiovascular Diseases* 2016; 5(1): 18–25, https://doi.org/10.17802/2306-1278-2016-1-18-25.